

Title	Microstructure evolution in dissimilar metal joint interface obtained by friction welding of cast iron and carbon steel
Author(s)	Ueji, Rintaro; Fujii, Hidetoshi; Ninomiya, Taketoshi et al.
Citation	Transactions of JWRI. 2013, 42(1), p. 33-37
Version Type	VoR
URL	https://doi.org/10.18910/26594
rights	
Note	

Osaka University Knowledge Archive : OUKA

<https://ir.library.osaka-u.ac.jp/>

Osaka University

Microstructure evolution in dissimilar metal joint interface obtained by friction welding of cast iron and carbon steel[†]

UEJI Rintaro*, FUJII Hidetoshi**, NINOMIYA Taketoshi **, MINO Akira ***

Abstract

The microstructure of the dissimilar joint between the ductile cast iron (JIS-FCD400) and the carbon steel (JIS-S45C) was studied in order to clarify the behaviors of the carbon diffusion and the plastic deformation. The interface of the joint consists of four different areas with different microstructures: (i) spheroidized graphite with a similar diameter to the base metal of the cast iron; (ii) the multi phased structure consisting of ferrite, pearlite and spheroidized graphite; (iii) pearlite only; (iv) ferrite and pearlite structure which is similar to the base metal of the carbon steel. The analysis of the Si distribution, the zones (i), (ii) and (iii) were included in the cast iron and (iv) lied in the carbon steel. The formation mechanism of the these microstructures was explained by the diffusion of carbon from the cast iron to the carbon steel and the inhomogeneous distribution of temperature. The misorientation measurement by the electron backscattering diffraction clarified that the area near the interface, which is the boundary between (iii) and (iv), was exposed to plastic deformation.

KEY WORDS: friction welding, microstructure, dissimilar joint, cast iron, carbon steel

1. Introduction

Friction welding is categorized as a the solid state joining process¹⁾. In friction welding, the base metals are contacted with a rotation and an applied load so that frictional heat evolves at the interface. After the adequate increase of temperature, an upset stress is additionally applied to obtain the sound joint. The stress during the FSW provides the plastic deformation as well. In that sense, the friction welding can be considered as a kind of plastic working process. Since the friction welding has several advantage such as lower cost due to the lower heat input, it is utilized in a wide field of industry²⁾. One of the characteristics of the friction welding is the good applicability for the dissimilar welding¹⁾. For example for steel joints, the friction welding is applied not only the similar joints of the plain carbon steel^{3,4)} or stainless steel⁵⁾ but also the dissimilar joint between carbon steel and stainless steel⁶⁾. The studies about these joints reported the relation between the welding parameter and mechanical properties⁴⁾ as well as the change of the micro hardness near the joint interface³⁾, however, the research works about the joint mechanism along with microstructure observations are limited.

By the way, friction stir welding (FSW) is another method for solid state joining. Recently, the application of the FSW has been extended to various materials

including steels^{7,8)}; Meanwhile, the detailed analysis of the microstructures in the FSW joint by the electron backscattering diffraction (EBSD)⁹⁾ has been conducted aggressively. These results are clarifying the relationship between the welding parameter and the mechanical properties of the joints along with the metallography. However, such a metallurgical approach has not been examined enough for the friction welding.

Consequently, this study aims to evaluate the microstructure in the friction welded dissimilar joint between the ductile cast iron (JIS-FCD400) and the carbon steel (JIS-S45C) both of which are the most used commercially, in order to clarify the metallurgical phenomena during the joining.

2. Experimental procedures

Ductile cast iron, JIS-FCD400 (2.4%C -3.1%Si - 0.96%Mn -bal.Fe) and the carbon steel, JIS-S45C (0.46mass%C -0.20%Si -bal.Fe) were used in this study. The shape of both samples were cylindrical bar with a diameter of 40mm. Friction welding was carried out using a pressure servo-control system brake type device. The welding parameters were a rotation speed of 2000rpm, a friction time of 10sec, a upset pressure of 100MPa and a upset time of 25sec. The microstructure of the joint was examined by a scanning

[†] Received on July 8, 2013

* Associate Professor

** Professor

***Murakami Seisakusho Co. Ltd.

Transactions of JWRI is published by Joining and Welding Research Institute, Osaka University, Ibaraki, Osaka 567-0047, Japan

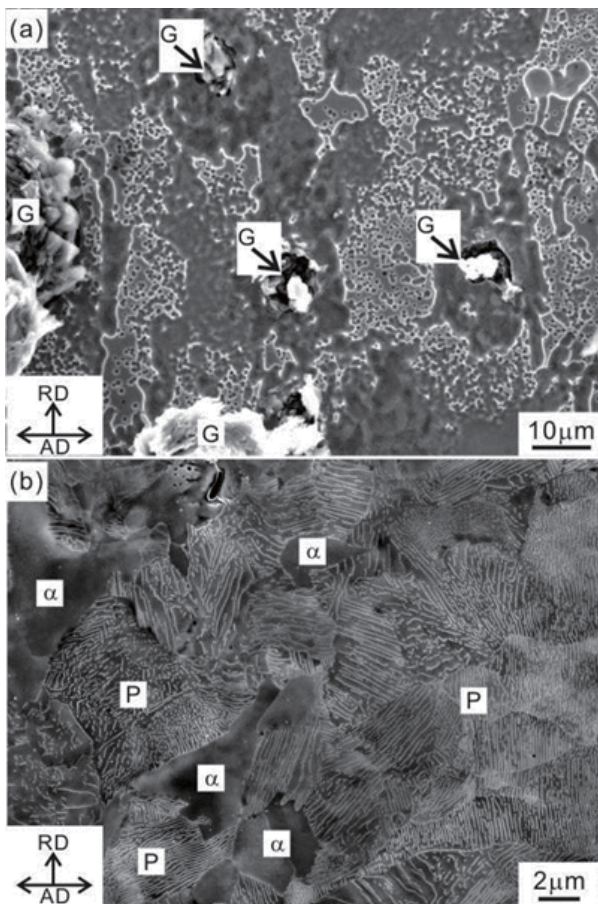


Fig. 1 SEM microstructures in the base metals of FCD (a) and S45C (b)

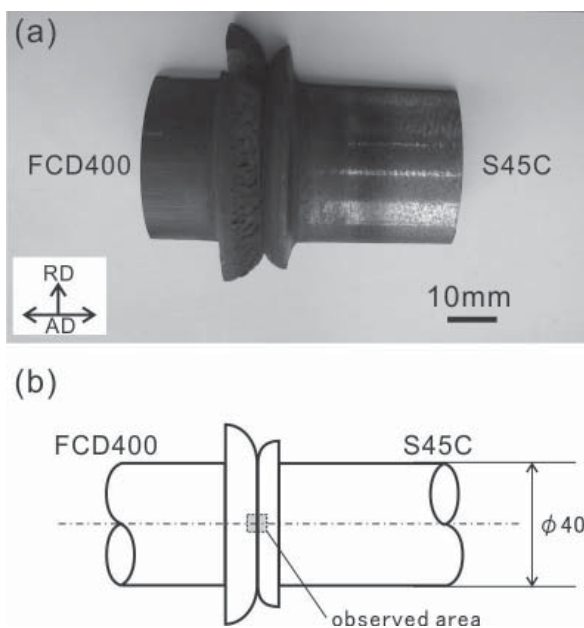


Fig. 2 Appearance (a) and schematic illustration (b) of the joint between FCD iron (left side) and S45C (right side)

electron microscope (SEM) and a transmission electron microscope (TEM). SEM was equipped with an EBSD system and an energy dispersion spectrometry (EDS) system to measure the spatial distribution of crystallographic orientations and alloying elements. Both the specimens for SEM and TEM observations were prepared by the electro polishing to observe the longitudinal sectional surface.

3. Results and Discussion

Figure 1 shows the SEM microstructures in the base metals of FCD (a) and S45C (b) samples. The horizontal and vertical directions on these images are parallel to the axial direction (AD) and the radius direction (RD), respectively. The base metal of the FCD sample show the spheroidized graphite with a diameter ranging from 5 μm to 20 μm . In the SC sample the mixture of ferrite (α) and the pearlite (P). These microstructures are typical for a ductile cast iron and carbon steel.

Figure 2 (a) shows the appearance of the joint between FCD iron (left side) and S45C (right side). The upset pressure provides some flash at the interface. There is no welding defect, indicating that a sound joint can be obtained at the selected joint parameter.

Figure 3 shows the SEM microstructures at the area indicated in Fig.2(b). The image at relatively low magnification is shown in Fig.3(a) and the enlarged image taken from the position (b), (c) and (d) are exhibited as well. These microstructures were observed at the axis center axis of the cylindrical bar. The SEM observation clarified that the joint area consists of 4 different zones with different microstructures. In this paper, these zones are referred as zones (i), (ii), (iii) and (iv) which align from the FCD iron side to the S45C steel side. The zone (i) has the spheroidized graphite structure which is just the same as that in the base metal of the FCD iron. In the zone (ii), which lies on the vicinity of the zone (i), the graphite was refined to a grain size of about 3 μm and the matrix was changed to the multi phased structure composed of the ferrite (α) and the pearlite. It should be noted that this mixture cannot be explained by the equilibrium phase diagram of Fe-C alloy system. Additionally, in the zone (iii), the spheroidized graphite disappears and only the pearlite structure can be observed. In the zone (iv) which locates at the most S45C steel side, the conventional ferrite and pearlite structure can be found.

Figure 4 shows the SEM microstructure (a) and the distribution maps of carbon (b) and silicon (c) of the area including the zones (ii), (iii) and (iv). The distribution maps were obtained by EDS measurements and the intensity of EDS signal was exhibited by the density of white points. As can be seen in the carbon map (b), the places indicating the higher carbon content are well corresponding with the positions of graphite;

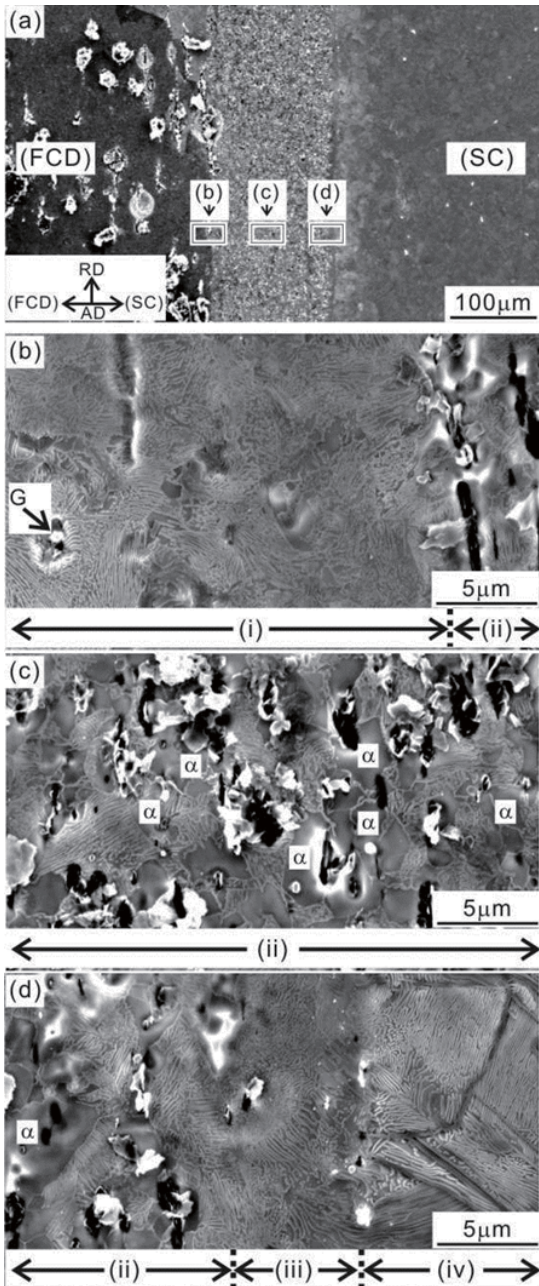


Fig. 3 SEM microstructures at the area indicated in Fig.2(b). The image at relatively low magnification is shown in Fig.3(a) and the enlarged image taken from the position (b), (c) and (d) are exhibited.

whereas the absence of silicon can be found at the zone (iv). This result indicates the original position of the interface. Since the chemical composition of the FCD iron is much higher than that of the S45C steel, the boundaries between (iii) and (iv) should be the original interface of the base metals.

Figure 5 shows the SEM images (a,b) and ferrite orientation color maps (c,d) of the joint at the area around the joint interface between the zones (iii) and (iv) (a,c) and the base metal of the S45C steel (b,d).

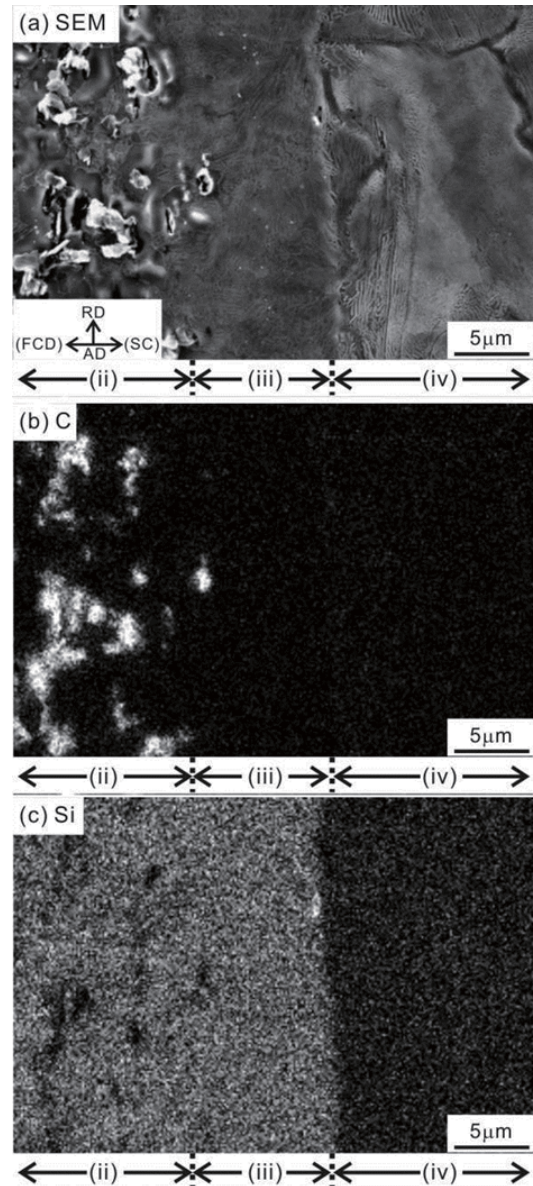


Fig. 4 SEM microstructure (a) and the distribution maps of carbon (b) and silicon (c).

The orientation color maps (c,d) show the crystallographic orientations parallel to the AD by the color code indicated in the standard triangles. The gray points indicate the area not available for the EBSD measurements. Additionally, the black line indicates the boundaries whose misorientation angle, θ , is higher than 0.75° . The morphology of pearlite in the joint interface (a) shows the complicated flow lines; whereas that in the base metal of the S45C steel (b) indicates relatively straight lines. The EBSD measurements clarified that the area around the (iii)/(iv) joint interface has much higher density of the low angle boundaries than that of the base metal of the S45C steel. These results indicate that the (iii)/(iv) joint interface was exposed to the plastic deformation by the upset stress.

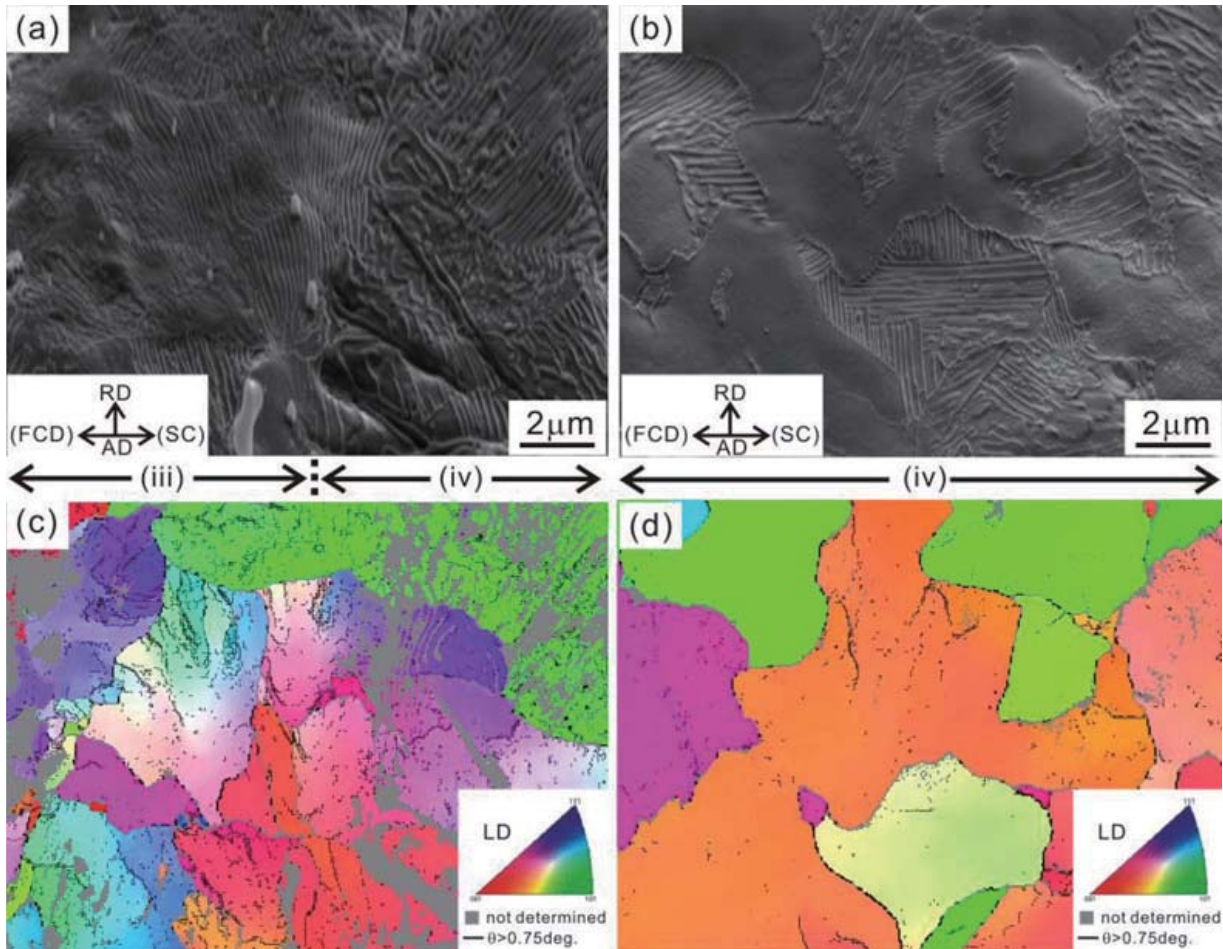


Fig. 5 SEM images (a,b) and ferrite orientation color maps (c,d) of the joint at the area around the joint interface between the zones (iii) and (iv) (a,c), and the base metal of the S45C steel (b,d).

It is because the misorientation is caused by the dislocation which can be found in the TEM observation of the joint as shown in **Fig.6**. Additionally, the size of pearlite colony of the (iii)/(iv) interface is larger than that of the S45C steel base metal. This implies the austenite grain refinement due to the deformation in austenite state.

As mentioned so far, this study clarified the complex microstructure at the interface of the dissimilar joint between the FCD cast iron and the S45C carbon steel. One of the characteristic features is that the area at the FCD cast iron side near the interface has both the zones with (ii) and without graphite (iii). This suggests the large temperature gradient in the joints. The zone (iii) has the higher peak temperature enough for the full austenitization due to the shorter distance from the interface, so that the diffusion of carbon happens at the austenite single phase condition; whereas, the zone (ii) has lower peak temperature and the diffusion of carbon takes place mainly at the austenite and graphite two phase regions. This can provide the multi phased structure which is

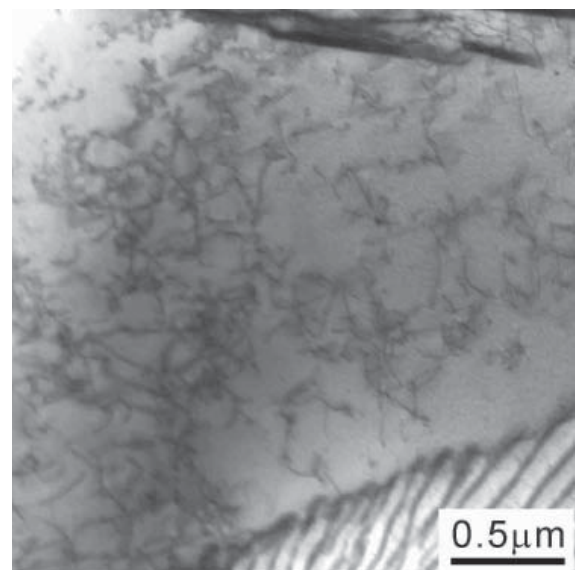


Fig. 6 TEM bright field image of the dissimilar joint between FCD cast iron and S45C carbon steel.

unpredictable from the equilibrium phase diagram.

Mater., 56 (2008) 2602-2614.

4. Conclusions

This study clarifies The microstructure of the dissimilar joint between the ductile cast iron (JIS-FCD400) and the carbon steel (JIS-S45C). The formation mechanism of the microstructures near the joint interface was explained by the diffusion of carbon from the cast iron to the carbon steel and the inhomogeneous distribution of temperature. The misorientation measurement by the electron backscattering diffraction clarified that the area near the interface was exposed to plastic deformation.

Acknowledgements

The authors wish to acknowledge the financial support of the Japan Science and Technology Agency (JST) under Collaborative Research Based on Industrial Demand “Heterogeneous Structure Control: Towards Innovative Development of Metallic Structural Materials”, a Grant-in-Aid for the Global COE Programs from the Ministry of Education, Sports, Culture, Science, and a Grant-in-Aid for Science Research from the Japan Society for Promotion of Science and Technology of Japan and ISIJ Research Promotion Grant.

References

- 1) M.B. Uday, M.N. Ahmad Fauzi, H. Zuhailawati and A.B. Ismail, Advances in friction welding process: a review, *Sci. Tech. Weld. Join.*, 15 (2010) 534-558.
- 2) V. Balasubramanian, Y. Li, T. Stotler, J. Crompton, A. Soboyejo, N. Katsube and W. Soboyejo, A New Friction Law for the Modelling of Continuous Drive Friction Welding: Applications to 1045 Steel Welds, *Mater. Manuf. Process.*, 14 (1999) 845-860.
- 3) W. Li and F. Wang, Modeling of continuous drive friction welding of mild steel, *Mater. Sci. Eng. A*, 528 (2011) 5921-5926.
- 4) M. Şahin and H.E. Akata, Joining with friction welding of plastically deformed steel, *J. Mater. Process. Tech.*, 142 (2003) 239-246.
- 5) P. Sathiya, S. Aravindan and A. Noorul Haq, Mechanical and metallurgical properties of friction welded AISI 304 austenitic stainless steel, *Int. J. Adv. Manufact. Tech.*, 26 (2005) 505-511.
- 6) N. Özdemir, Investigation of the mechanical properties of friction-welded joints between AISI 304L and AISI 4340 steel as a function rotational speed, *Mater. Lett.*, 59 (2005) 2504-2509.
- 7) H. Fujii, L. Cui, N. Tsuji, M. Maeda, K. Nakata and K. Nogi, Friction stir welding of carbon steels, *Mater. Sci. Eng. A*, 429 (2006) 50-57.
- 8) L. Cui, H. Fujii, N. Tsuji and K. Nogi, Friction stir welding of a high carbon steel, *Scr. Mater.*, 56 (2007) 637-640.
- 9) S. Miroov, Y.S. Sato and H. Kokawa, Microstructural evolution during friction stir-processing of pure iron, *Acta*